

Supplementary Materials for  
“Symmetry-Breaking Drop Bouncing on Superhydrophobic Surfaces with  
Continuously Changing Curvatures”

WooSeok Choi and Sungchan Yun

Department of Mechanical Engineering, Korea National University of Transportation, Chungju 27469,  
Republic of Korea

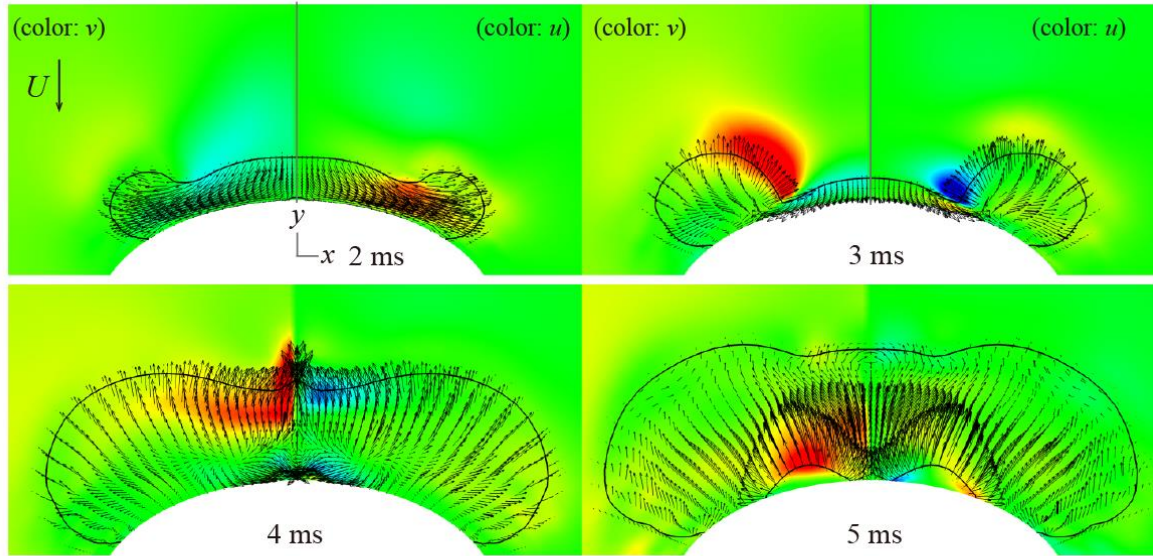
S2: Figure S1. Velocity field distributions of  $e^+$  and  $e^-$  drops.

S3: Figure S2. Momentum asymmetry on several surfaces at the constant  $\kappa_0$ .

S4: Figure S3. Shape evolutions of the oblate ellipsoidal drops on  $E$ -surfaces.

S5: Figure S4. Shape evolutions of 45°-rotated ellipsoidal drops on  $E$ -surfaces.

(a)  $e^+$  drops



(b)  $e^-$  drops

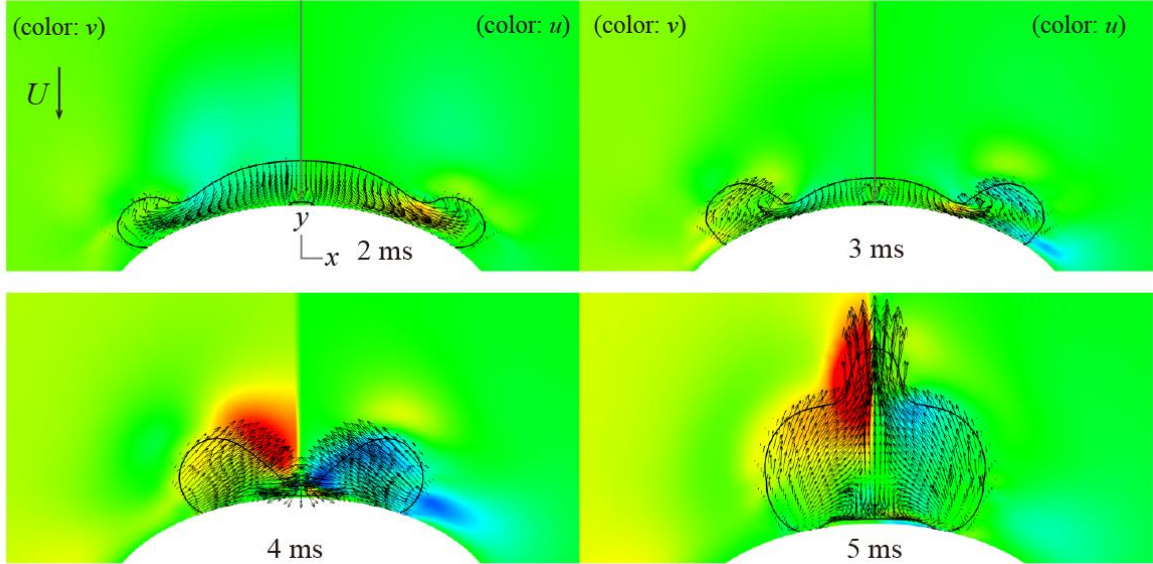


Figure S1. Velocity field distributions (arrow) and the magnitude of the velocity (color) of the drops with (a)  $e = +0.45$  and (b)  $e = -0.45$  on  $E(2.0, 1.2)$  surfaces at  $We = 24$ .  $U$ ,  $u$ , and  $v$  correspond to the initial impact velocity,  $x$ -velocity, and  $y$ -velocity, respectively. The left and right columns of the contours represent the  $v$  and  $u$ , respectively. The intensity of the color is clipped at the initial impact velocity  $\pm U$  (red: high; blue: low).

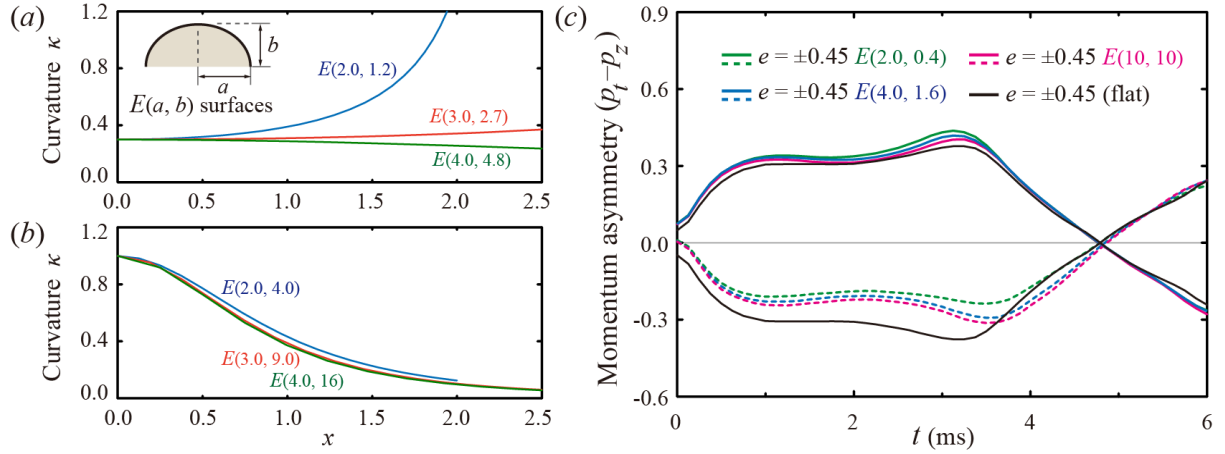


Figure S2. Dimensionless curvature  $\kappa$  along the  $x$  axis at the initial surface curvature of (a)  $\kappa_0 = 0.3$  and (b)  $\kappa_0 = 1.0$ . The high deviation of  $\kappa$  between the surfaces at the low  $\kappa_0$ , whereas the slight deviation of  $\kappa$  between the surfaces at the high  $\kappa_0$ . (c) Temporal variations of the momentum asymmetry ( $p_t - p_z$ ) at  $e = +0.45$  (solid line) and  $e = -0.45$  (dashed line) on the surfaces at  $\kappa_0 = 0.1$ . The momentum asymmetries on several  $E$ -surfaces, including the  $E(10, 10)$  surfaces, are comparable to each other.

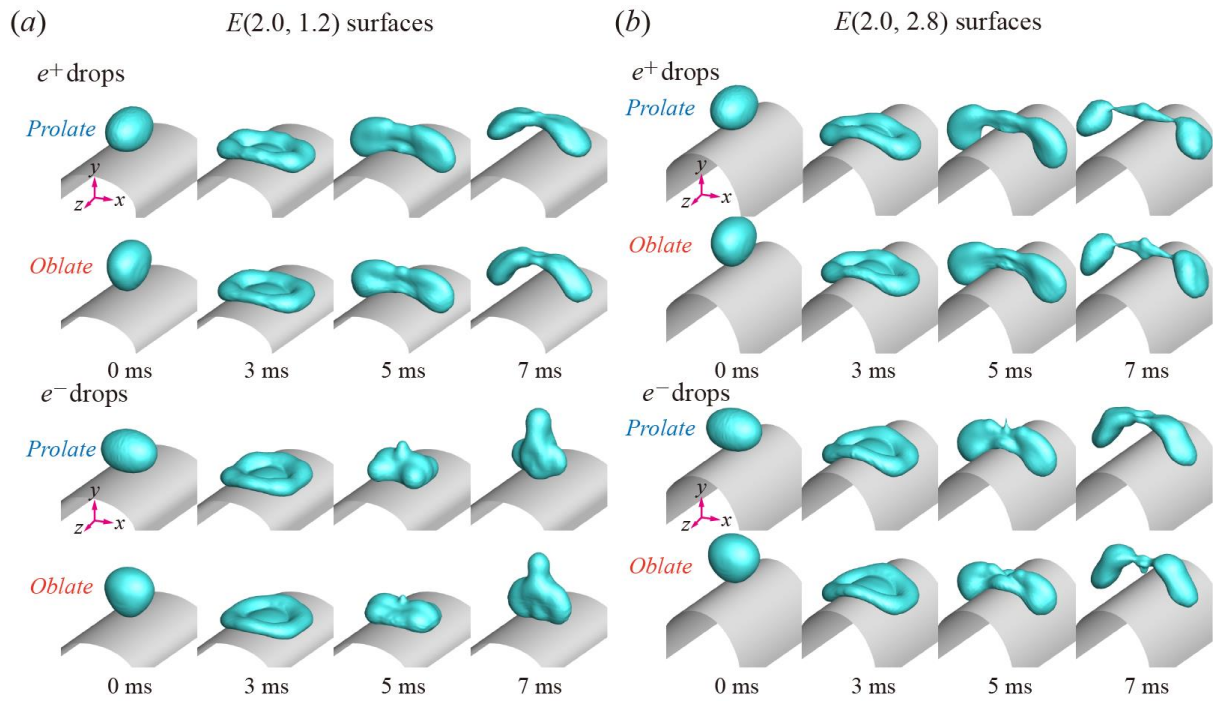
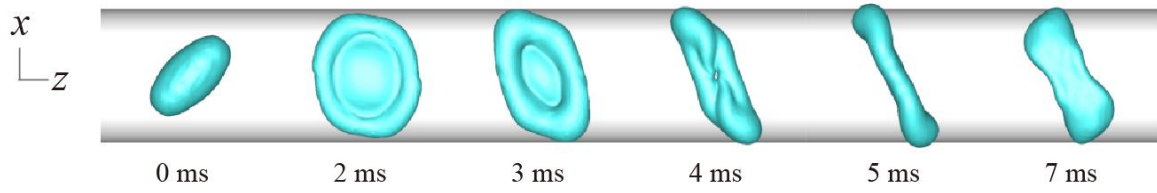


Figure S3. Bouncing dynamics on (a)  $E(2.0, 1.2)$  and (b)  $E(2.0, 2.8)$  surfaces for prolate and oblate spheroidal drops with  $e = \pm 0.25$  at  $We = 24$ . The shape evolution and residence time of the prolate drops are comparable to those of the oblate drops.

(a)  $E(2.0, 1.2)$  surfaces



(b)  $E(2.0, 2.8)$  surfaces

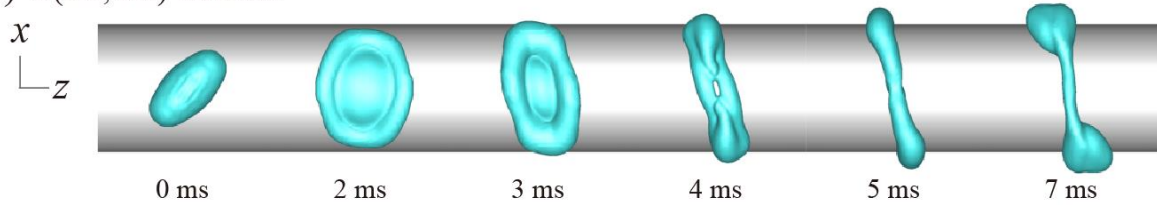


Figure S4. Snapshots of the bouncing dynamics of  $45^\circ$ -rotated prolate drops around the  $y$  axis on (a)  $E(2.0, 1.2)$  and (b)  $E(2.0, 2.8)$  surfaces at  $We = 24$ . The drops complete the liquid alignment along the direction biased slightly to the  $x$  axis because of a pronounced flow to the axis induced by the curvature, as shown at 5 ms. The drops leave the  $b1.2$  and  $b2.8$  surfaces at 5.3 and 5.2 ms, respectively.